

## A Contrast Based Image Fusion Technique Using Digital Shearlet Transform and Root Mean Square Contrast

<sup>1</sup>R. Adaline Suji, <sup>1</sup>D. Bright Anand and <sup>2</sup>R. Saravanan

<sup>1</sup>Department of Computer Science and Engineering,  
Ratnavel Subramaniam College of Engineering and Technology, Dindigul, Tamilnadu, India  
<sup>2</sup>R.V.S Educational Trust's Group of Institutions, Dindigul, Tamilnadu, India

**Abstract:** The process of combining methodology from more images into a single highly contrasted image is called as image fusion. A highly contrasted image extracts the best of input images then conveying into the single image. Image fusion has many applications to get the proper solutions in Satellite imaging, Digital imaging, Medical imaging, Multi-focus imaging etc. Image registration process performs to transform different coordinate systems into one coordinate system. A contrast based image fusion technique is introduced using digital shearlet Transform (DST). A digital shearlet transform utilized for multi resolution decomposition of input images. Since the image sharpness is measured using contrast. The low band coefficients of digital shearlet transform are selected based on the contrast level. The noise represented high band coefficients of digital shearlet transform is selected based on root mean square (RMS) contrast. Then, fuse both low and high band coefficients. Final fused image gets by inverse of the digital shearlet transform. The results of the proposed method gives better Correlation Coefficients (CC), Root Mean Square Error (RMSE), Relative Average Spectral Error (RASE) and Erreur Relative Globale Adimensionnelle de Synthese (ERGAS) values as compare with Wavelet Transform (WT), Dual Tree Continuous Wavelet Transform (DTCWT), Curvelet Transform (CT), Contourlet Transform (CLT) fusion techniques.

**Key words:** Image Fusion • Digital Shearlet Transform • Contrast Level • Root Mean Square Contrast

### INTRODUCTION

The image fusion [1-3] is nothing but the collection input images combined into a single output image which contains a better description of the scene than the one provided by any of the individual input images. The output image is more useful for human visual perception or machine perception. To fuse images, image registration plays an important role to set the different coordinate systems of images into single coordinate system. Researchers have proposed that multi-scale transform [4-5] based fusion techniques. In multi-scale transforms, at first, the wavelet domain is developed an image fusion technique. The Wavelet Transform [6-7] is a popular transform for image processing. Wavelet Transform is transformed into sub-groups by exerting the multi resolution decomposition techniques. However, wavelets won't get the smoothness along the contours.

Curvelet [8] is another multi-scale transforms technique, which executes easier, simple and speedier than the wavelet techniques. The drawback is that it avoids a direct transition from the continuum to the digital setting. The Contourlet Transform [9-10] consists of two primary steps for image decomposition technique: Laplacian Pyramid (LP) decomposition and Directional Filter Bank (DFB) decomposition. LP technique is decomposed the image into low band and high band images. And its high band image is decomposed by DFB. Contourlet transform holds the directionality and anisotropy. However, the computational complexity is too high and continuum theory is discarded in this approach.

Shearlet Transform [11-12] is the most successful technique for the multidimensional data efficient representation. One of the distinctive characteristics of shearlets is that the utilization of shearing to control directional selectivity, rather than rotation utilized by

curvelets. The Shearlet Transform consolidates the power of multi-scale methods to capture the geometry of multidimensional information and is ideally proficient in images containing edges. In shearlet transform, the Discrete Shearlet Transform (DST) is extremely focused on performance and computational efficiency of the denoising applications.

In this paper, the low band coefficients of DST have selected for the contrast level. The noise representing high band coefficients of DST have selected specific pixel as an edge if both of the image pixels have same contrast level. Fuse the low band and high band coefficients then inverse of the digital shearlet transform.

This paper can be followed as: Section II characterizes the discrete shearlet transform, Section III describes the proposed fusion method, Section IV discusses the experimental results and Section V summarizes the conclusion of this paper.

**Discrete Shearlet Transform:** Basically, shearlets are composite wavelengths  $L^2(\mathbb{R}^2)$ , which are well localized, optimally sparse and satisfy parabolic scaling. Each element  $\hat{\Psi}_{j,l,k}^{(d)}$  supports a pair of trapezoids. And each element is contained  $2^j \times 2^{2j}$  size, shown in Figure 1.

The Discrete Shearlet Transform is most convenient to depict the collection of shearlets presented above properties. Its numerical implementation can be defined as follows. For  $\mathcal{D}_0 = \{(\xi_1, \xi_2) \in \mathbb{R}^2, |\xi_1| \geq \frac{1}{8}, \frac{|\xi_2|}{|\xi_1|} \leq 1, j \neq 0\}$  and  $l = -2^j, \dots, 2^j - 1$ , let  $\hat{\Psi}^{(0)}$  is defined as.

$$\hat{\Psi}^{(0)}(\xi) = \hat{\Psi}^{(0)}(\xi_1, \xi_2) = \hat{\Psi}_1(\xi_1) \hat{\Psi}_2\left(\frac{\xi_2}{\xi_1}\right) \tag{1}$$

$$W_{j,l}^{(0)}(\xi) = \begin{cases} \hat{\Psi}_2\left(2^j \frac{\xi_2}{\xi_1} - 1\right) \chi_{\mathcal{D}_0}(\xi) + \hat{\Psi}_2\left(2^j \frac{\xi_2}{\xi_1} - 1 + 1\right) \chi_{\mathcal{D}_1}(\xi) & \text{if } l = -2^j \\ \hat{\Psi}_2\left(2^j \frac{\xi_2}{\xi_1} - 1\right) \chi_{\mathcal{D}_0}(\xi) + \hat{\Psi}_2\left(2^j \frac{\xi_2}{\xi_1} - 1 - 1\right) \chi_{\mathcal{D}_1}(\xi) & \text{if } l = 2^j - 1 \\ \hat{\Psi}_2\left(2^j \frac{\xi_2}{\xi_1} - 1\right) & \text{otherwise} \end{cases} \tag{2}$$

And  $\mathcal{D}_1 = \{(\xi_1, \xi_2) \in \mathbb{R}^2, |\xi_2| \geq \frac{1}{8}, \frac{|\xi_2|}{|\xi_1|} \leq 1\}$ , then  $\hat{\Psi}^{(1)}$  is defined as

$$\hat{\Psi}^{(1)}(\xi) = \hat{\Psi}^{(1)}(\xi_1, \xi_2) = \hat{\Psi}_1(\xi_2) \hat{\Psi}_2\left(\frac{\xi_1}{\xi_2}\right) \tag{3}$$

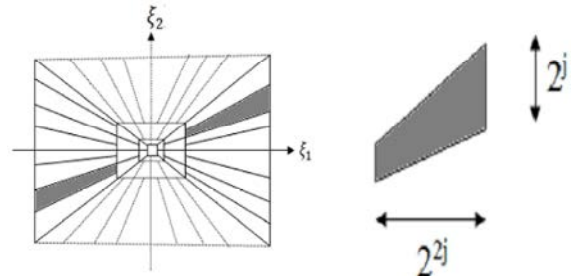


Fig. 1: Tiling frequency of shearlets and frequency support of shearlets

$$W_{j,l}^{(1)}(\xi) = \begin{cases} \hat{\Psi}_2\left(2^j \frac{\xi_2}{\xi_1} - 1\right) \chi_{\mathcal{D}_0}(\xi) + \hat{\Psi}_2\left(2^j \frac{\xi_2}{\xi_1} - 1 + 1\right) \chi_{\mathcal{D}_1}(\xi) & \text{if } l = -2^j \\ \hat{\Psi}_2\left(2^j \frac{\xi_2}{\xi_1} - 1\right) \chi_{\mathcal{D}_0}(\xi) + \hat{\Psi}_2\left(2^j \frac{\xi_2}{\xi_1} - 1 - 1\right) \chi_{\mathcal{D}_1}(\xi) & \text{if } l = 2^j - 1 \\ \hat{\Psi}_2\left(2^j \frac{\xi_2}{\xi_1} - 1\right) & \text{otherwise} \end{cases} \tag{4}$$

Where  $\Psi_2 \in [-1,1]$ . For  $l = -2^j \leq l \leq 2^j - 1$ , here  $W_{j,l}^{(d)}(\xi)$  is a window function on a pair of trapezoids, illustrated as Figure 1(a). When  $l = -2^j$  or  $l = 2^j - 1$ , at the junction of the horizontal cone and vertical cones  $\mathcal{D}_0$  and  $\mathcal{D}_1$ ,  $W_{j,l}^{(d)}(\xi)$  is the superposition of two such functions.

Using this notation, for  $j \geq 0, -2^j \leq l \leq 2^j - 1, k \in \mathbb{Z}, d = 0,1$ , we can write the Fourier transform of the shearlets in the equation (5)

$$\hat{\Psi}_{j,l,k}^{(d)}(\xi) = 2^{\frac{3j}{2}} V(2^{-2j}\xi) W_{j,l}^{(d)}(\xi) e^{-2\pi i \xi A_d^{-j} B_d^{-1} k} \tag{5}$$

Where,

$$V(\xi_1, \xi_2) = \hat{\Psi}_1(\xi_1) \chi_{\mathcal{D}_0}(\xi_1, \xi_2) + \hat{\Psi}_2(\xi_2) \chi_{\mathcal{D}_1}(\xi_1, \xi_2)$$

the dilation matrices  $A^j, B^j$  are associated with scale transformations, area-preserving geometrical transformations respectively, such as rotations and shear.

$$A_0 = \begin{pmatrix} 4 & 0 \\ 0 & 2 \end{pmatrix}, B_0 = \begin{pmatrix} 1 & 1 \\ 0 & 1 \end{pmatrix}, A_1 = \begin{pmatrix} 2 & 0 \\ 0 & 4 \end{pmatrix}, B_1 = \begin{pmatrix} 1 & 0 \\ 1 & 1 \end{pmatrix} \tag{6}$$

The digital shearlet transform of  $f \in L^2(\mathbb{R}^2)$  can be computed as

$$SH_{\Psi} f(a, s, t) = \langle f, \Psi_{j,l,k}^{(d)} \rangle = 2^{\frac{3j}{2}} \int_{\mathbb{R}^2} \hat{f}(\xi) \overline{V(2^{-2j}\xi) W_{j,l}^{(d)}(\xi)} e^{2\pi i \xi A_d^{-j} B_d^{-1} k} d\xi \tag{7}$$

Certainly, one can easily verify that

$$\sum_{d=0}^1 \sum_{l=-2j}^{2j-1} |W_{j,l}^{(d)}(\xi_1, \xi_2)|^2 = 1 \tag{8}$$

And from equation (8), it follows that

$$|\hat{\varphi}(\xi_1, \xi_2)|^2 + \sum_{\substack{d=0 \\ \in \mathbb{R}^2}}^1 \sum_{j=0}^{\infty} \sum_{l=-2j}^{2j-1} |V(2^{2j}\xi_1, 2^{2j}\xi_2)| |W_{j,l}^{(d)}(\xi_1, \xi_2)|^2 = 1 \text{ for } (\xi_1, \xi_2) \in \mathbb{R}^2 \tag{9}$$

**MATERIALS AND METHODS**

In this paper, the proposed fusion method obtains the contrast fused image from the two image sources, shown in Figure 2. To achieve this method, the following steps describe to obtain the contrast fused image.

- First of all, read the images from  $I_1$  and  $I_2$  image sources and computes its size in rows and columns wise.
- Intensity based image registration is utilized. Because it registers entire images or sub-images and correspond feature points in images
- DST domain local direction band limited contrast at  $m^{\text{th}}$  scale and  $n^{\text{th}}$  direction.  $SH_{LF}^{I_1}(i, j)$ ,  $SH_{LF}^{I_2}(i, j)$  and  $SH_{m,n}^{I_1}(i, j)$ ,  $SH_{m,n}^{I_2}(i, j)$  are the low band and high band coefficients of the image sources  $I_1$  and  $I_2$  respectively.

$$I_1(i, j) = SH_{LF}^{I_1}(i, j) + \sum_{m,n} SH_{m,n}^{I_1}(i, j)$$

$$I_2(i, j) = SH_{LF}^{I_2}(i, j) + \sum_{m,n} SH_{m,n}^{I_2}(i, j)$$

- For selecting low band coefficient, the contrast level measurement can be defined as

$$Contrast = \frac{\text{bandwidth coefficient}}{\text{lowpass band coefficient}}$$

Here the bandwidth coefficient can be represented the value of an input image pixel.  
Hence

$$I_{c_1}(i, j) = I_1(i, j) / SH_{LF}^{I_1}(i, j)$$

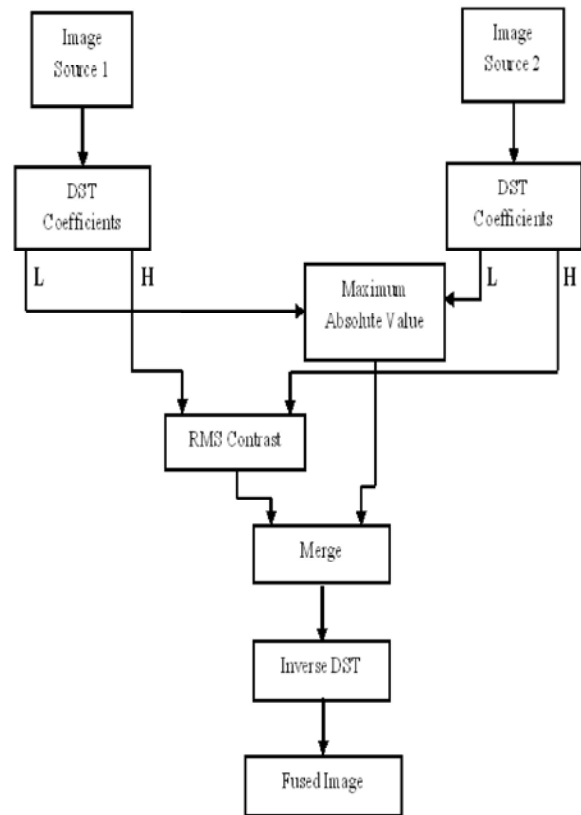


Fig. 2: Block diagram of proposed method using DST and Maximum absolute value and RMS contrast

$$I_{c_2}(i, j) = I_2(i, j) / SH_{LF}^{I_2}(i, j)$$

$$I_L(i, j) = \begin{cases} SH_{LF}^{I_2}(i, j) & \text{if } I_{c_1}(i, j) \geq I_{c_2}(i, j) \\ SH_{LF}^{I_1}(i, j) & \text{otherwise} \end{cases}$$

- The high band coefficient is selected based on the following procedure. The high band coefficient contains information about edges and contours. Since the noise is represented as high frequency components. If the pixels of the both images have better contrast pixel, then that particular pixel is selected as edge. Root mean square (RMS) contrast can be utilized by the standard deviation of the input pixel intensities, which does not depend on the spatial distribution of contrast in the image. The RMS contrast of an image can be defined as

$$I_R = \sqrt{\frac{1}{MN} \sum_{i=0}^{M-1} \sum_{j=0}^{N-1} (I_{i,j} - \bar{I})^2}$$

Where  $I_{ij}$  is the  $i^{th}$  and  $j^{th}$  element of the two dimensional image of size  $M$  by  $N$ .  $\bar{I}$  is an average intensity of each and every pixel value of that image. Hence, by utilizing the RMS contrast, the high band coefficients of the better pixel value can be defined as

$$I_L(i, j) = \begin{cases} SH_{m,n}^{I_1}(i, j) & \text{if } I_{R_1} \geq I_{R_2} \\ SH_{m,n}^{I_2}(i, j) & \text{otherwise} \end{cases}$$

Where  $I_{R_1}$ ,  $I_{R_2}$  are the RMS contrasts of the images  $I_1, I_2$  respectively.

- And merge both low band and high band coefficients.
- Finally get the fused image  $I_f$  by inverse of the DST.

### RESULT AND DISCUSSION

In this section, the experiment results demonstrated after implemented the proposed fusion technique. As per Table 1, CC, RMSE, RASE and ERGAS to evaluate the fusion result in this paper. Table 2 describes that the CC, RMSE, RASE and ERGAS of fused images are compared

Table 1: Metrics for performance evaluation of different images

Metrics for performance	Equation	Properties
Correlation Coefficients (CC)	$CC = \frac{\sum_{i=1}^m \sum_{j=1}^n (I_r(i, j) - \bar{I}_r) (I_f(i, j) - \bar{I}_f)}{\sqrt{\sum_{i=1}^m \sum_{j=1}^n (I_r(i, j) - \bar{I}_r)^2 \sum_{i=1}^m \sum_{j=1}^n (I_f(i, j) - \bar{I}_f)^2}}$ <p>Where <math>I_r(i, j), I_f(i, j)</math> represent the reference image, fused images and <math>\bar{I}_r, \bar{I}_f</math> represent the mean values of the reference and fused images</p>	The correlation coefficient of reference and fused image is regularly utilized to indicate their degree of correlation. The best value of correlation coefficient is 1.
Root Mean Square Error (RMSE)	$RMSE(B_i) = \sqrt{\frac{1}{MN} \sum_{i=1}^M \sum_{j=1}^N (I_r(i, j) - I_f(i, j))^2}$ <p>M is the mean radiance of the N spectral bands (<math>B_i</math>) of the original Multi Spectral bands,</p>	Calculated the root mean square error of the reference image $I_r$ and the fused image $I_f$ .
Relative Average Spectral Error (RASE)	$RASE = \frac{100}{M} \sqrt{\frac{1}{N} \sum_{i=1}^N RMSE^2(B_i)}$	RASE is used to estimate the spectral quality of the fused images as a percentage by characterizing the average performance of the image fusion in the spectral bands.
Erreur Relative Globale Adimensionnelle de Synthèse (ERGAS)	$ERGAS = 100 \frac{h}{l} \sqrt{\frac{1}{N} \sum_{i=1}^N \frac{RMSE^2(B_i)}{M_i^2}}$ <p>Where <math>M_i</math> represents the mean radiance of each multispectral band in the fusion and <math>h, l</math> represent the high and low spatial resolutions of the images.</p>	ERGAS is calculated for comparison the spectral quality and spatial quality of the different fused images. Spatial quality is approximated by the edges sharpness whereas the spectral quality is done with many matrices.

Table 2: Comparison between Previous Fusion Techniques and Proposed Method

	Image 1			
	CC	ERGAS	RASE	RMSE
Wavelet Transform	0.037	2.65	10.83	41.32
DTCWT	0.033	2.52	10.04	40.01
Curvelet Transform	0.030	2.26	9.58	37.25
Contourlet Transform	0.025	2.10	8.65	31.58
PROPOSED	0.022	1.85	7.22	29.17
	Image 2			
	CC	ERGAS	RASE	RMSE
Wavelet Transform	0.124	9.26	35.46	39.95
DTCWT	0.107	8.44	31.81	32.65
Curvelet Transform	0.065	6.41	20.24	24.76
Contourlet Transform	0.043	4.92	14.53	15.11
PROPOSED	0.024	3.24	11.25	13.42

Table 2: Continue

Image 3				
	CC	ERGAS	RASE	RMSE
Wavelet Transform	0.017	6.18	21.30	26.68
DTCWT	0.015	5.71	15.88	21.25
Curvelet Transform	0.006	4.24	10.25	15.66
Contourlet Transform	0.004	3.12	9.22	10.79
PROPOSED	0.002	2.20	7.88	9.71
Image 4				
	CC	ERGAS	RASE	RMSE
Wavelet Transform	0.052	2.99	11.09	44.02
DTCWT	0.050	2.57	10.16	40.30
Curvelet Transform	0.041	2.01	9.76	37.11
Contourlet Transform	0.032	1.87	8.54	30.55
PROPOSED	0.026	1.70	7.14	27.01
Image 5				
	CC	ERGAS	RASE	RMSE
Wavelet Transform	0.029	3.09	11.61	45.58
DTCWT	0.025	2.88	10.68	41.94
Curvelet Transform	0.023	2.14	9.54	35.67
Contourlet Transform	0.021	1.98	8.71	31.54
PROPOSED	0.019	1.87	7.61	29.85
Image 6				
	CC	ERGAS	RASE	RMSE
Wavelet Transform	0.112	4.04	15.16	55.52
DTCWT	0.104	3.49	14.07	51.52
Curvelet Transform	0.088	2.87	13.54	39.69
Contourlet Transform	0.067	2.58	10.08	36.66
PROPOSED	0.053	2.37	9.60	35.44

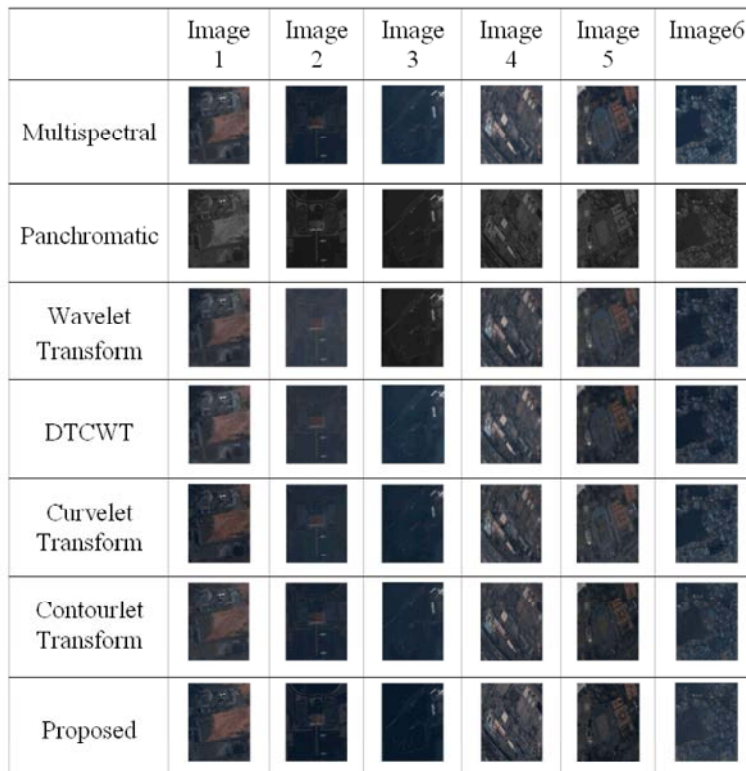


Fig. 3: Resultant Images based on DWT, DTCWT, Curvelet, Contourlet and Proposed techniques.

with the other fusion techniques. Based on DST and RMS contrast, Experiment results show that the CC, RMSE, RASE and ERGAS of the proposed fusion technique is better than the other fusion techniques of WT, DTCWT, CT and CLT, shown in Figure 3.

### CONCLUSION

This paper proposes a contrast based image fusion technique utilizing the digital shearlet transform and RMS contrast. The low band coefficients of DST are selected by the contrast level. The high band coefficients of digital shearlet transform are selected by RMS contrast. Then the resultant low band coefficients and high band coefficients are fused. And final fused image is obtained by inverse of the digital shearlet transform. Experiment states that the CC, RMSE, RASE and ERGAS of the proposed method gives better results as compared with Wavelet-based, DTCWT-based, Curvelet-based, Contourlet -based fusion techniques.

### REFERENCES

1. Simone, G., A. Farinab, F.C. Morabito, S.B. Serpico and L. Bruzzone, 2002. Image fusion techniques for remote sensing applications, Elsevier Science, pp: 3-15.
2. Rick. S. Blum and Zheng liu, 2005. multi-sensor image fusion and its applications Taylor & Francis group, CRC Press, London, United Kingdom.
3. Goshtasby Ardeshir and Stavri Nikolov, 2007. Image fusion: Advances in the state of the art Elsevier, pp: 114-118.
4. Murtagh F. 1998. Multiscale Transform Methods in Data Analysis, pp: 1-8.
5. Jean-Luc-Starck, Michael Elad and David Donoho, 2004. Redundant multiscale transforms and their application for morphological component separation, Elsevier, pp: 1-64.
6. Hui Li, B.S. Manjunath and Sanjit K. Mitra, 1994. multi-sensor image fusion using the wavelet transform, IEEE transaction, 51-55.
7. Hai-Hui Wang, Jun Wang and Wei Wang, 2005. Multispectral Image Fusion Approach based on GHM Multi Wavelet.
8. Guangming Zhang, Zhiming Cui, Li Fanzhang and Wu. Jian, 2009. DSA Image Fusion Based on Dynamic Fuzzy Logic and Curvelet Entropy, Journal Of Multimedia, 4(3): 129-136.
9. Zhuangzheng Zhao and YunXiangLi, 2010. A Novel Image Fusion Method Based on Fuzzy Contourlet Transform, IEEE International Conference on Computer and Communication Technologies in Agriculture Engineering, pp: 404-407.
10. Minh N. Do and Martin Vetterli, 2005. The Contourlet Transform: An Efficient Directional Multiresolution Image Representation, IEEE Transactions on Image Processing, 14(12): 2091-2106.
11. GittaKutyniok, Demetrio Labate, 2012. Introduction to Shearlets, Applied and Numerical Harmonic Analysis, pp: 1-38.
12. Kutyniok G. and J.Lemvig, 2012. Compactly Supported Shearlets, Springer Proceedings in Mathematics, 13:163-186.